ELSEVIER

Journal of Nuclear Materials 294 (2001) 168–174

journal of nuclear materials

www.elsevier.nl/locate/jnucmat

X-ray photoelectron spectroscopy on uranium oxides: a comparison between bulk and thin layers

S. Van den Berghe [a,*], F. Miserque [b], T. Gouder [b], B. Gaudreau [c], M. Verwerft [a]

[a] *SCK-CEN, Reactor Materials Research, Boeretang 200, B-2400 Mol, Belgium*

[b] *European Commission, JRC, Institute for Transuranium Elements, Postfach 2340, D-76125 Karlsruhe, Germany*

[c] *Université de Limoges, SPCTS UMR-CNRS no. 6638, Av. Albert-Thomas, 87060 Limoges cedex, France*

Abstract

The use of sputter deposited thin layers of UO_2 as a model system for the investigation of fuel–fission product interactions is presented. The representativity of the layers for the bulk system will be validated and it will be shown, both on theoretical and experimental grounds, that layers of stoichiometric UO_2 can be produced by this method. A comparison will be made between X-ray photoelectron spectroscopic (XPS) results on bulk UO_2 and on the deposited layers. The films deposited can easily be doped with other elements, such as fission products, by codepositing these elements with the UO_2. This codeposition technique has subsequently been used to produce layers of UO_2 containing cesium. It will be demonstrated that the codeposition with cesium produces uranium in higher valence states (up to U^{VI}), while without cesium, no higher uranium valencies can be obtained. © 2001 Elsevier Science B.V. All rights reserved.

1. Introduction

Over the past decades, much research has been performed to investigate the interaction between nuclear fuels and the fission products. In view of the complexity of the fuel–fission product system, much effort has been put into the conception of model systems to study the interactions in a controlled fashion.

In this paper, an approach to model system engineering with a sputter deposition technique is presented. The results of an X-ray photoelectron spectroscopy (XPS) study of in situ deposited layers of UO_2 of various stoichiometries will be discussed. The spectra of the layers that are considered to consist of pure UO_2, are shown to compare well with the results obtained on the bulk system. Furthermore, a theoretical approach, proving the stoichiometry of the thin layers, is presented. Because of the flexibility of the deposition technique, these thin layers can easily be doped with fission products and, as the technique is in situ, the resulting films can be studied using XPS without exposure to uncontrolled atmospheres. To demonstrate this flexibility, codeposited layers of UO_2 doped with cesium have been produced by introduction of a cesium vapour in the preparation chamber during the deposition.

2. Experimental

The thin films were prepared in situ by DC sputtering (4×10^{-3} mbar Ar, U metal target at −500 V). The plasma in the triode source is maintained by injection of electrons of 50–100 eV energy coming from a heated W filament. This setup was previously used in other deposition experiments [1] and will be described in detail in a forthcoming paper. The current flowing from the target to the substrate is monitored and taken as a measure for the deposition speed. This value can be varied by tweaking the deposition parameters (Ar pressure, high voltage settings, current through the W filament, ...). As a sputter gas, ultrahigh purity Ar (99.9999%) was used. All depositions were performed at room temperature.

When oxygen is required, analytical grade oxygen is fed through a leak valve into the preparation chamber for reactive sputter depositions or directly into the

* Corresponding author. Tel.: +32-14 333 064; fax: +32-14 321 216.

E-mail address: svdbergh@sckcen.be (S. Van den Berghe).

0022-3115/01/$ - see front matter © 2001 Elsevier Science B.V. All rights reserved.
PII: S 0 0 2 2 - 3 1 1 5 (0 1) 0 0 4 6 1 - 5

analysis chamber for oxygen exposures. The pressure measurements are performed through a port in the chamber and are therefore only indications of the true pressures at the level of the substrate. Because of local pressure build-ups, the values quoted in this paper will not necessarily correspond to the values obtained in other setups, but they were recorded consistently throughout this work and their relative values are therefore relevant. Cesium vapour was generated using outgassed SAES getter sources placed in close proximity to the substrate. All specimens containing cesium were prepared under the same conditions (oxygen pressure, sputter parameters, temperature, ...) as required for the production of stoichiometric UO_2 thin layers.

All thin layer spectra were recorded at the Institute for Transuranium Elements using a Leyboldt LHS-10 hemispherical analyser with a pass energy of 50 eV. XPS spectra were recorded with MgKα (1253.6 eV) radiation. X-ray satellites were subtracted numerically. UPS measurements were performed using HeII (40.81 eV) radiation from a windowless UV rare gas discharge source. In UPS the total resolution was 0.1–0.05 eV. In the analysis chamber, the background pressure was 1.5×10^{-10} mbar, while in the preparation chamber pressures of 4×10^{-9} mbar could be sustained. As a substrate, monocrystalline Si was chosen because of its good compatibility with the deposited uranium oxide layers. The substrates were cleaned before introduction in the spectrometer and heated to about 400°C for several hours before use.

For the preparation of a bulk UO_2 sample, a pellet was sintered for 48 h under an Ar + 5% H_2 atmosphere at 1450°C. The pellet was broken before mounting in the sample holder and stored in vacuum after mounting.

The instrument used for XPS measurements of the bulk sample was a Physical Electronics ESCA Model 1600 from the University of Brussels (Metallurgy Dept.), with a non-monochromated Al X-ray source, operated at 400 W. A description of the system and acquisition parameters can be found in [2].

For the X-ray diffraction (XRD) measurements, a Philips X'Pert Pro goniometer was used. The instrument is equipped with an X-ray mirror for thin film analysis allowing the recording of the spectra without the influence of the underlying substrate. The library of PDF-data files was used to compare the recorded peak positions to known UO_2 positions.

3. Results

3.1. Deposition of UO_2 thin layers

In order to determine the oxygen partial pressure required in the preparation chamber to deposit stoichiometric UO_2, layers at various oxygen pressures from 0 to 5×10^{-4} mbar were produced and their photoelectron spectra were examined. At the highest pressure, it proved difficult to ignite the plasma, so no attempt was made to go to higher pressures. These difficulties arise from the fact that the metallic uranium target oxidises too fast, which hinders the formation of the DC electric field that is required to form the plasma.

In Fig. 1, the valence band spectra are depicted. For the layers that are produced without addition of oxygen in the chamber, the typical spectrum of metal [3–5] is obtained with the sharp U5f peak at the Fermi level. Even in the UHV of 10^{-10} mbar, a slight oxidation of the surface of the metallic uranium cannot be avoided. This can be seen in Fig. 1 from the slight onset of the U–O-bonding band around 5.7 eV. Upon introduction of 1×10^{-5} mbar of oxygen during deposition, the U–O bonding band develops further. Also observable is the appearance of the U5f peak at 2.4 eV that belongs to the two remaining 5f electrons in the U atoms that are bound to oxygen [6]. With increasing oxygen pressure, the U–O bonding band develops further and the U5f peak at 2.4 eV grows at the expense of the U5f peak at the Fermi level. At oxygen pressures above 5×10^{-5} mbar, the metallic U5f peak disappears and subsequently, the entire spectrum shifts toward lower binding energies. At 1×10^{-4} mbar, the maximal shift of 1.1 eV is reached and the U5f peak is found at 1.35 eV. Higher oxygen pressures do not change the spectrum any further.

An analogous behaviour is observed in the core level region of the U4f peaks that are displayed in Fig. 2. Without the presence of oxygen, only the metallic U4f peaks are recorded at 388.0 eV for the $U4f_{5/2}$ and 377.2 eV for the $U4f_{7/2}$. They are very sharp (FWHM = 1.6 eV) and highly asymmetric, as described in the literature [3–5]. Upon introduction of oxygen in the sputtering atmosphere, the two U4f peaks that belong to the oxidised uranium develop at 391.8 and 380.9 eV. At the

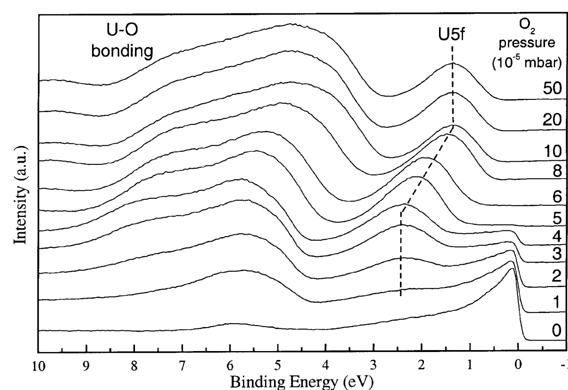

Fig. 1. Valence band spectra of thin films deposited at varying oxygen partial pressures.

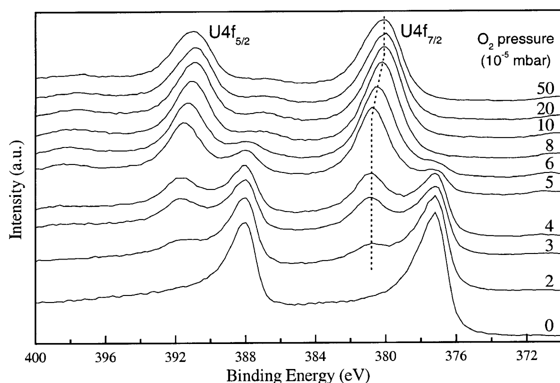

Fig. 2. U4f spectra of thin films as a function of the partial oxygen pressure in the preparation chamber during deposition.

same time, the shake-up satellite peak appears at about 6.8 eV distance from these main peaks, At 6×10^{-5} mbar partial oxygen pressure, the metallic uranium peaks have completely disappeared. The remaining intensity at the position of the $U4f_{5/2}$ metal peak is due to the shake-up satellite of the $U4f_{7/2}$ peak of the oxidised species. As in the case of the valence band, the spectra of the layers that were deposited at oxygen pressure above 5×10^{-5} mbar shift towards lower binding energies. At 1×10^{-4} mbar oxygen partial pressure, the typical U4f signal of UO_2 is obtained and the peaks remain stationary at 390.9 and 380.1 eV.

The spectra from layers, deposited at a partial oxygen pressure of 1×10^{-4} mbar, can now be compared to the spectra of bulk UO_2, recorded on a different spectrometer. For stoichiometric UO_2, peak positions of 380.0 and 390.8 eV are found for the $U4f_{7/2}$ and $U4f_{5/2}$ peaks, respectively, as can be seen in Fig. 3. The characteristic shake-up satellites are observed at 6.7 eV to the high

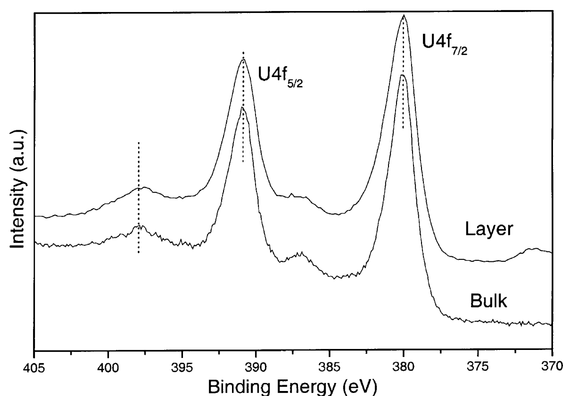

Fig. 3. Comparison of the U4f spectra of UO_2 in bulk and in thin layer. Keep in mind that both the spectra were recorded on different spectrometers The binding energy values and widths of different photoelectron peaks are displayed in Table 1.

Table 1
Comparison of the binding energy values, peak widths and satellite positions for the bulk and the thin film UO_2 sample[a]

	Thin layer (eV)	Bulk (eV)
$U4f_{5/2}$	390.9	390.8
FWHM	2.1	<2.0
$U4f_{7/2}$	380.1	380.0
Satellite	6.8	6.7
O1s	530.1	530.0
U5f	1.35	1.3

[a] Keep in mind that both the spectra were recorded on different spectrometers.

binding energy side of the main peaks, as described in the literature [2,7]. The peak width amounts to 2.0 eV and was determined solely for the $U4f_{7/2}$ peak because the $U4f_{5/2}$ peak is broadened by the satellite from the $U4f_{7/2}$ peak. In the valence band region, the U5f peak is found at 1.3 eV. On the bulk samples, the valence band (VB) was recorded using X-ray-induced VB spectroscopy, because no UV-lamp is mounted on this spectrometer. Therefore, only binding energy information can be compared. The binding energy values of the U4f, O1s and U5f peaks for both the thin layers and the bulk sample are reproduced in Table 1 for comparison, while Fig. 3 displays the U4f spectra of both samples.

Using XRD, it was determined that the deposited layers are crystalline. The recorded XRD spectra show the diffractrion lines corresponding to UO_2.

3.2. Codeposition experiments

By allowing cesium vapour in the preparation chamber during the sputter deposition of uranium, codeposited layers can be produced. The resulting thin layer contains both uranium and cesium in an amount that depends on their deposition speeds. The deposition speed of UO_2 was kept constant by monitoring the current flowing from the metallic uranium target to the substrate and keeping it at about 3 mA, resulting in a deposition speed of around 2 ML/s (monolayers per second). The deposition speed of cesium was varied by changing the current flowing through the getter source from 6 to 7.5 A in steps of 0.5 A. Because the deposition speed was observed to vary from one experiment to the other at the same current, no values for the deposition speed with each current can be given, but the amounts of cesium and uranium in the produced layers can be estimated afterwards using the XPS signal intensity ratios. This results in 33 at.% U (no Cs), 23 at.% U with 10 at.% Cs (6 A), 19 at.% U with 17 at.% Cs (6.5 A), 14 at.% U with 27 at.% Cs (7 A) and 10 at.% U with 40 at.% Cs (7.5 A) balanced by oxygen. The XPS spectra of U4f, Cs3d, O1s and the valence band were monitored.

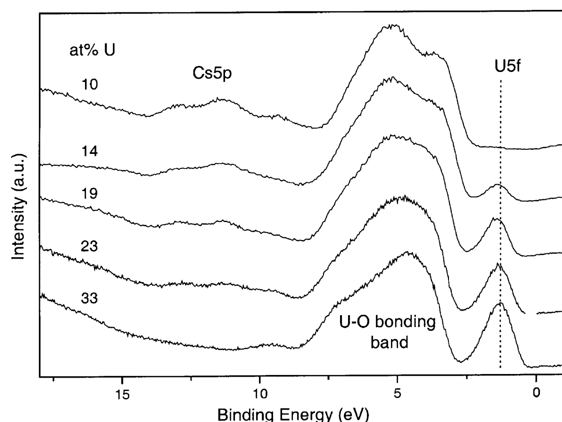

Fig. 4. Valence band spectra of cesium–uranium codeposited thin layers as a function of the current through the cesium getter source. The uranium content of the samples is indicated in at%. Note the complete disappearance of the U5f signal at the highest cesium deposition speed.

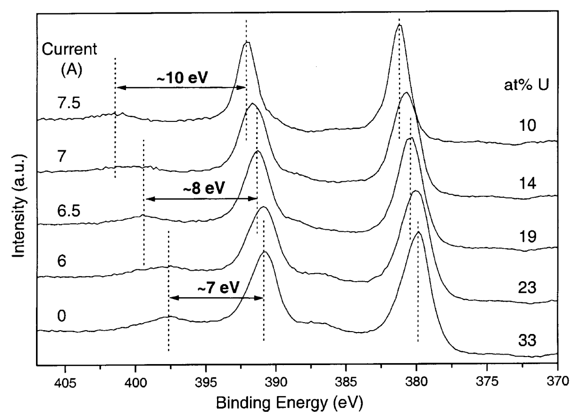

Fig. 5. U4f spectra of codeposited films as a function of the current through the cesium getter source. The clear shift of the U4f main peaks, accompanied by the change in the satellite position, indicates formation of U^{VI} at the highest cesium deposition rate. Note the extraordinary small width of the peaks.

A clear change in the valence band spectra with increasing cesium content is visible in Fig. 4 as the U5f peak intensity diminishes markedly. This reduction of the intensity is, of course, in part due to the dilution of the uranium by the presence of cesium. However, this effect cannot account for the entire reduction and a true disappearance of the U5f signal is even observed when a current of 7.5 A is used. At the same time, the Cs5p peaks develop at 11.4 and 13.0 eV and the appearance of a feature that is superposed on the U–O bonding band around 5 eV can be observed. This peak is linked to another one that is very weakly visible at around 9.5 eV binding energy on top of the U–O bonding band. These peaks were always observed to grow or diminish together.

Looking at the U4f signals in Fig. 5, a shift of these peaks towards the high binding energy side is observed as more cesium is added. The initial peak position of 390.9 eV of the $U4f_{5/2}$ peak shifts to 391.0 eV for 6 A, 391.3 eV for 6.5 A, 391.7 eV for 7 A and 392.1 eV for 7.5 A. At the same time, the shake-up satellite at the high binding energy side shifts from 6.8 eV distance to around 8 eV distance from the main peak at 6.5 A and finally to 10 eV distance at 7.5 A. The width of the main peaks also diminishes with the amount of cesium added, from 2.1 eV for pure UO_2 to 1.7 eV for 7.5 A, which is extremely sharp.

For the Cs3d signal, no real evolution except the logical increase in intensity is seen. The peaks are found at 738.9 eV for $Cs3d_{3/2}$ and 724.9 eV for $Cs3d_{5/2}$, which are the known positions for oxidised Cs. At the low cesium concentrations, the influence of the $U4d_{5/2}$ line at 739 eV can still be seen. The O1s position is stationary at 530.1 eV, although a significant broadening of this signal is observed at higher cesium concentrations. Its width goes from 1.6 eV for pure UO_2 to 2.3 eV at 7.5 A caused by the developed asymmetry of the peak towards the high binding energy side because of the presence of another O1s peak.

4. Discussion

4.1. Deposition of UO_2 thin layers

As a first requirement for studying the influence of cesium doping on uranium dioxide thin layers, one needs to be able to deposit thin layers of stoichiometric UO_2. Because UO_2 is known to readily deviate from stoichiometry, a technique to assess the stoichiometry of a deposited layer has to be found. Fortunately, a noticeable change in the electronic properties of uranium oxide, visible by XPS, occurs when it changes from hypo- to hyperstoichiometric.

Theoretically, UO_2 of perfect stoichiometry is a so-called Mott–Hubbard insulator [8]. The addition or removal of oxygen atoms in the lattice causes the creation of electrons or holes in the valence band that allow electronic conductivity, whereas for stoichiometric UO_2, these are created by thermal disproportionation [9,10] according to

$$2U^{4+} \rightarrow U^{5+} + U^{3+}.$$

The statistical probability of this reaction $\delta = e^{F/2kT} = e^{(1\ \mathrm{eV}/kT)-1}$ is the so-called intrinsic disorder parameter (with free energy $F = 2$ eV-2kT). On the basis of this probability relation, it can be seen that the disproportionation does not play a role at room temperature

($\delta = 4.3 \times 10^{-17}$ at 300 K). Even the slightest hyperstoichiometry (one oxygen atom per dm^2 per monolayer) will cause a larger effect on the conductivity than the disproportionation. At higher temperatures, however, δ increases and the disproportionation plays a more important role than the stoichiometry for small deviations from stoichiometry (notably in the region $|x| < \delta$) [10]. In hyperstoichiometric UO_{2+x}, the excess oxygen atoms act as electron acceptor impurities that remove electrons from the UO_2 valence band [10]. As a consequence, the hyperstoichiometric uranium oxides are p-type semiconductors. On the other hand, the hypostoichiometric uranium oxide is an n-type semiconductor [10,11]. Therefore, at room temperature, a transition from n- to p-type semiconductivity will occur at $x = 0$.

For an n-type semiconductor, the Fermi level E_f lies near the bottom of the conduction band, while for a p-type E_f is found near the top of the valence band [12]. In XPS, the Fermi level of the sample will always be in balance with that of the spectrometer, provided the sample is grounded and sufficiently conductive [12,13]. Consequently, a switch from n- to p-type semiconduction will produce core-level shifts the size of the band gap as the Fermi level remains fixed at the E_f of the spectrometer and the bands will be displaced by the creation of an electrostatic potential [12]. This change in semiconductor type (n to p) can thus be observed in the XPS spectra of Figs. 1 and 2 as a shift of all peaks to lower binding energies with the change in the position of the Fermi level. Such binding energy shifts have been observed for other semiconductors as well [14,15]. Effects such as band bending and the existence of surface states can complicate the behaviour of the Fermi level, but for a highly ionic semiconductor such as $UO_{2\pm x}$, these surface effects are negligable.

As the band gap for UO_2 was determined to be 2.1–2.7 eV [10,11,16], the Fermi level shift of 1.1 eV as observed in our experiment does not agree with the size of the band gap. This is accounted for by the fact that in the sputtered layer, large amounts of defect states will be present, that will pin the Fermi level somewhere in between the top of the valence band and the bottom of the conduction band. This result cannot therefore be used to determine the size of the band gap in UO_2.

As an additional check of the stoichiometry, a comparison of the spectra recorded from the thin films to those from bulk samples is imperative. The different binding energy values for both samples are summarised in Table 1 and the U4f spectra are compared in Fig. 3. There is a very good agreement of both U4f peak positions (less than 0.1 eV difference). Even the FWHM of the thin film U4f peaks (2.1 eV) is relatively close to the widths obtained on the bulk material (<2.0 eV), considering the fact that the resolution that was used to record the spectra of the thin films was inherently less good than for the other XPS, partly because pass energy values of 50 eV were used for the thin layer analyses compared to the 5 eV for the bulk samples. The satellite positions agree very well, also within 0.1 eV, as do the O1s binding energies.

The binding energy values for the bulk UO_2 ($U4f_{7/2}$ at 380.0 eV and $U4f_{5/2}$ at 390.8 eV) agree quite perfectly with the binding energies recorded by Allen et al. [17] on a $UO_{2.001}$ pellet ($U4f_{7/2}$ at 380.0 eV and $U4f_{5/2}$ at 390.8 eV) but our peaks have slightly smaller widths (<2.0 eV compared to 2.1 eV). The agreement with results on monocrystalline UO_2 [7] is also quite good ($U4f_{7/2}$ at 380.15 eV and $U4f_{5/2}$ at 391.00 eV). Agreement with the results found in [18] ($U4f_{7/2}$ at 380.3 eV and $U4f_{5/2}$ at 391.2 eV) is less good, but the UO_2 in this reference was formed by oxidation of U metal and its stoichiometry is therefore doubtful, especially in view of the results obtained on the thin layers, where higher binding energies are also recorded for substoichiometric samples. From out better values for the FWHM (2.0 eV compared to 2.6 eV), our samples are thought to be closer to stoichiometry than those taken in this reference. Also, the values reported in [2] deviate markedly from what is reported here. This is entirely due to the charging correction that was applied. If the value of 285.1 eV is taken as the C1s binding energy instead of 284.6 eV, the values agree perfectly. The 284.6 eV adopted in the cited paper is the C1s binding energy for carbon on metals and should not be applied for the UO_2 ceramic.

Although it may seem surprising to find that there is no development of further hyperstoichiometry at higher partial oxygen pressures, a reasoning based on the kinetics of oxidation rationalises such a behvaiour. The kinetics of the oxidation of uranium metal will be much faster than the oxidation of a stable oxide such as UO_2. Comparing the literature data on oxygen exposures required to oxidise U metal to UO_2, to the exposures required to further oxidise a UO_2 surface, proves this point. In [6,18], it is stated that a stoichiometric UO_2 film is produced on a U metal surface by exposing it to 3×10^{-5} Torr of O_2 for 30 min or to 54×10^3 L (1 L = 1 Langmuir = 1 s exposure to 1×10^{-6} Torr O_2). Although no value is given for the thickness of the film and though it is believed that the surface layer is not completely stoichiometric, this exposure is small compared to the 120 h exposure to the same oxygen pressure (amounting to 1.3×10^7 L) that is subsequently required to oxidise this surface further. Even then, only a hyperstoichiometry of $x = 0.07 \pm 0.02$ is claimed. In [7], oxygen exposures of over 3×10^8 L are used to oxidise a sample of crystalline UO_2 and there also, the hyperstoichiometry is limited. In this study, a freshly prepared stoichiometric UO_2 thin film was exposed to pure oxygen up to 5000 L, without any changes whatsoever in the valence band spectrum. Even though the actual oxygen potential present in the preparation chamber during the deposi-

tion is more than adequate to produce higher oxides, the kinetics of the oxidation reaction beyond UO_2 are just too slow for such phases to form in the given time, taking into account that the deposition is readily performed at speeds of 2 ML/s (monolayers per second). Thus, the direct reactive sputter deposition of higher oxides of uranium beyond UO_2 is not possible by this method, since higher oxygen pressures would be required and these are limited by the oxidation of the target. Experimentally, this means that in situ deposited layers do not contain oxidation states of uranium higher than IV.

4.2. Codeposition experiments

In the codeposition experiments, the three elements cesium, uranium and oxygen are present together in the preparation chamber in varying ratios. As more cesium is added, keeping the uranium deposition rate constant, a clear evolution in the uranium XPS signal (Figs. 4 and 5) is visible. The U4f peaks shift to higher binding energies (1.2 eV shift from 390.9 to 392.1 eV for $U4f_{7/2}$, the shake-up satellites shift to larger separations from the main peak (from 6.7 to 10 eV) and the U5f peak intensity diminishes. Considering the disappearance of the U5f electron signal in the valence band and taking into account the U^{VI} signature that is observed in the U4f spectrum (main peaks at 381.2 and 392.1 eV and satellite at 10 eV separation [2,19]), it can only be concluded that U^{VI} has formed in the codeposition experiment at 7.5 A current through the getter source. Remembering the impossibility of producing higher oxides of uranium by our reactive sputter deposition set-up, even at the highest possible oxygen partial pressures, it is surprising to see that by adding the most electropositive element known, higher valences of uranium are formed. Cesium cannot directly cause this further ionisation of uranium, considering its chemical properties, thus a reaction mechanism has to be invoked in which the potential barrier for this oxidation beyond U^{IV} is lowered by the presence of cesium in some way. This reaction mechanism is currently being studied using layered structures. The codeposited layers will also be studied with X-ray diffraction.

It is possible that uranate species are formed when the hot atoms from the plasma are deposited on the substrate. As they are still very mobile, the uranium oxide can form crystal structures with the cesium atoms, thus forming uranates, but that does not resolve the problem why uranium oxidises more easily in the presence of cesium. If the XPS peak positions are compared to the positions known for cesium uranates in [2], some differences can be noticed. As stated earlier, the U4f peak positions recorded in [2] for bulk uranates were corrected for charging, meaning that these positions depend upon the value taken for the C1s binding energy, which should be higher than that mentioned in [2] (285.1 eV instead of 284.6 eV). The values quoted below are therefore corrected by 0.5 eV with respect to the values in [2]. The Cs3d positions differ markedly between the layers and the bulk samples. In the bulk case, the $Cs3d_{5/2}$ peak is found around 724.1 eV, while in the thin layers and value of 724.9 eV is found. For the U4f peaks, binding energies are closer to each other for both samples, with $U4f_{7/2}$ binding energy values of 381.2 eV in the case of the thin layers, and of 381.4–381.0 eV in the bulk case depending on the uranate phase taken. It should be pointed out that the U4f binding energy values of UO_3 are significantly higher than those found for U^{VI} here (382.0 eV [20] compared to the 381.2 eV found here), which points to the formation of a compound with the cesium. However, the difference between the Cs3d peak positions signifies that the bonding of the cesium atoms is different in both samples. Further research will be required to provide answers to this question, starting with XRD analysis of the codeposited layers.

5. Conclusion

It can be concluded that thin layers of uranium oxide deposited with a partial oxygen pressure of 1×10^{-4} mbar in our preparation chamber consist of stoichiometric, crystalline layers of UO_2. This can be deduced on theoretical grounds, in which the n-p-type semiconductor transition of the uranium oxide when passing from hypo- to hyperstoichiometry is taken as a reference. Comparison with bulk UO_2 leads to additional evidence for the stoichiometry of the thin layers. Furthermore, no higher oxides can be deposited because the kinetics of UO_2 oxidation are too slow and the experimentally attainable oxygen pressures are limited by the oxidation of the uranium metal that forms the target material. The properties of the thin stoichiometric layers, especially the electrochemical behaviour, will be investigated in detail in a forthcoming paper.

By introducing cesium vapour in the preparation chamber during deposition, an oxidation of the uranium from U^{IV} to U^{VI} was observed. The reaction mechanism causing this transformation is still under investigation. It is as yet undetermined if complexes are formed between the cesium and the uranium oxide or if the cesium catalyses the oxidation reaction.

Acknowledgements

We would like to thank the University of Brussels for the use of their XPS equipment.

References

[1] T. Gouder, J. Electr. Spectr. Rel. Phen. 101–103 (1999) 419.
[2] S. Van den Berghe, J.P. Laval, B. Gaudreau, H. Terryn, M. Verwerft, J. Nucl. Mater. 277 (2000) 28.
[3] S. Fujimori, Y. Saito, K. Yamaki, T. Okane, N. Sato, T. Komatsubara, S. Suzuki, S. Sato, Surf. Sci. 444 (2000) 180.
[4] T. Gouder, Surf. Sci. 382 (1997) 26.
[5] T. Gouder, C.A. Colmenares, J.R. Naegele, Surf. Sci. 342 (1995) 299.
[6] G.C. Allen, I.R. Trickle, P.M. Tucker, Philos. Mag. B 43 (4) (1981) 689.
[7] G.C. Allen, P.A. Tempest, J.W. Tyler, J. Chem. Soc. Faraday Trans. 1 83 (1987) 925.
[8] A. Kotani, T. Yamazaki, Physica B 186–188 (1993) 16.
[9] J.C. Killeen, J. Nucl. Mater. 88 (1980) 185.
[10] P.W. Winter, J. Nucl. Mater. 161 (1989) 38.
[11] B.W. Veal, D.J. Lam, Phys. Rev. B 10 (12) (1974) 4902.
[12] W.F. Egelhoff, Surf. Sci. Rept. 6 (1987) 253.
[13] D. Briggs, M.P. Seah (Eds.), Practical Surface Analysis, Vol. 1, Wiley, New York, 1990.
[14] G.S. Henshaw, V. Dusastre, D. Williams, J. Mater. Chem. 6 (8) (1996) 1351.
[15] H. Lüth, Surfaces and Interfaces of Solid Materials, Springer, Berlin, 1997.
[16] Y. Baer, J. Schoenes, Solid State Commun. 33 (1980) 885.
[17] G.C. Allen, J.A. Crofts, M.T. Curtis, P.M. Tucker, J. Chem. Soc. Dalton Trans. 1974 (1974) 1296.
[18] G.C. Allen, P.M. Tucker, J.W. Tyler, J. Phys. Chem. 86 (1982) 224.
[19] S. Bera, S.K. Sali, S. Sampath, S.V. Narasimhan, V. Venugopal, J. Nucl. Mater. 255 (1998) 26.
[20] G.C. Allen, N.R. Holmes, J. Chem. Soc. Dalton Trans. 1987 (1987) 3009.